
Robust Ante-hoc Graph Explainer using Bilevel Optimization

Kha-Dinh Luong

Department of Computer Science
University of California, Santa Barbara

Mert Kosan

Department of Computer Science
University of California, Santa Barbara

Arlei Lopes Da Silva

Department of Computer Science
Rice University, Houston

Ambuj Singh

Department of Computer Science
University of California, Santa Barbara

Abstract

Explaining the decisions made by machine learning models for high-stakes applications is critical for increasing transparency and guiding improvements to these decisions. This is particularly true in the case of models for graphs, where decisions often depend on complex patterns combining rich structural and attribute data. While recent work has focused on designing so-called post-hoc explainers, the broader question of what constitutes a good explanation remains open. One intuitive property is that explanations should be sufficiently informative to reproduce the predictions given the data. In other words, a good explainer can be repurposed as a predictor. Post-hoc explainers do not achieve this goal as their explanations are highly dependent on fixed model parameters (e.g., learned GNN weights). To address this challenge, we propose RAGE (Robust Ante-hoc Graph Explainer), a novel and flexible ante-hoc explainer designed to discover explanations for graph neural networks using bilevel optimization, with a focus on the chemical domain. RAGE can effectively identify molecular substructures that contain the full information needed for prediction while enabling users to rank these explanations in terms of relevance. Our experiments on various molecular classification tasks show that RAGE explanations are better than existing post-hoc and ante-hoc approaches.

1 Introduction

A critical problem in machine learning on graphs is understanding predictions made by graph-based models in high-stakes applications. This has motivated the study of graph explainers, which aim to identify subgraphs that are both compact and correlated with model decisions. However, there is no consensus on what constitutes a good explanation. Recent papers [39, 23, 3] have proposed different alternative notions of explainability that do not consider the user and instead are validated using examples. Other approaches have applied labeled explanations to learn an explainer directly from data [8]. However, datasets with such labeled explanations are hardly available.

Explainers can be divided into *post-hoc* and *ante-hoc* (or *intrinsic*) [32]. Post-hoc explainers treat the prediction model as a black box and learn explanations by modifying the input of a pre-trained model [42]. On the other hand, ante-hoc explainers learn explanations as part of the model. Figure 2 compares the post-hoc and ante-hoc approaches in the context of graph classification. The key advantage of post-hoc explainers is their flexibility since they make no assumption about the prediction model to be explained or the training algorithm applied to learn the model. However, these explanations have two major limitations: (1) they are not sufficiently informative to enable the user to reproduce

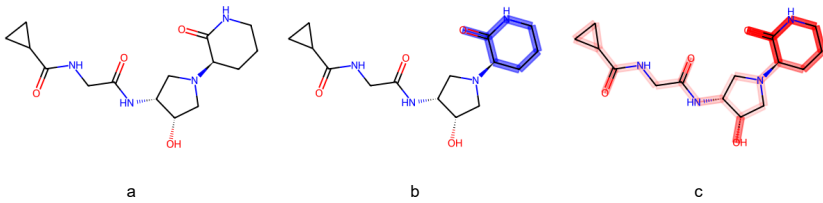


Figure 1: An example of explanations generated by our approach (RAGE) on molecular graphs from the synthetic dataset LACTAM. Subfigure (a) shows an input molecule, subfigure (b) highlights the ground-truth explanation and subfigure (c) illustrates the edge weights assigned by RAGE. Our method correctly identified the subgraph corresponding to the ground-truth lactam functional group.

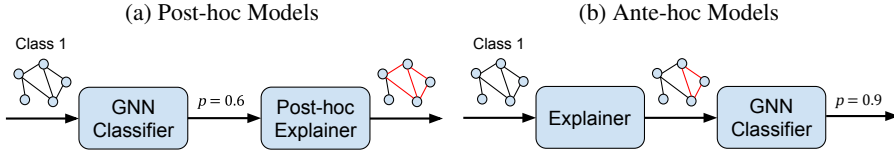
the behavior of the model, and (2) they are often based on a model that was trained without taking explainability into account.

The first limitation is based on the intuitive assumption that a good explanation should enable the user to approximately reproduce the decisions of the model for new input. That is simply because the predictions will often depend on parts of the input that are not part of the post-hoc explanations. The second limitation is based on the fact that for models with a large number of parameters, such as neural networks, there are likely multiple parameter settings that achieve similar values of the loss function. However, only some of such models might be explainable [28, 45]. While these limitations do not necessarily depend on a specific model, this paper addresses them in the context of Graph Neural Networks (GNNs) for graph-level classifications.

This paper proposes RAGE, a novel ante-hoc explainer for graphs that finds compact explanations while maximizing the graph classification accuracy using bilevel optimization. RAGE explanations are given as input to the GNN, which guarantees that no information outside of the explanation is used for prediction. We show that RAGE explanations are more robust to noise in the input graph than existing (post-hoc and ante-hoc) alternatives. Moreover, our explanations are learned jointly with the GNN, which enables RAGE to learn GNNs that are accurate and explainable. In fact, we show that RAGE’s explainability objective produces an inductive bias that often improves the accuracy of the learned GNN compared to the base model. We emphasize that while RAGE is an ante-hoc model, it is general enough to be applied to a broad class of GNNs.

Figure 1 shows an example of RAGE explanations on an input molecule from LACTAM, one of our semi-synthetic molecular datasets. The goal is identifying whether the molecule contains lactam functional groups, which are cyclic amides of various ring sizes. Figure 1b shows the molecule with the ground-truth explanation highlighted in blue. Figure 1c illustrates the edge influences learned by RAGE, with darker shades of red indicating higher weights or more important edges. As expected, edges corresponding to the ground-truth explanation received distinguishably higher weights. We show more examples of explanations by RAGE in Appendix E. Our main contributions can be summarized as follows:

- We highlight and empirically demonstrate two important limitations of post-hoc graph explainers. They do not provide enough information to enable reproducing the behavior of the predictor and are based on fixed models that might be accurate but not explainable.
- We propose RAGE, a novel GNN and flexible explainer for graph classifications. RAGE applies bilevel optimization, learning GNNs in the inner problem and an edge influence function in the outer loop. Our approach is flexible enough to be applied to a broad class of GNNs.
- We compare RAGE against state-of-the-art graph classification and GNN explainer baselines using 8 datasets—including 5 real-world ones. RAGE not only performs competitively or better compared to the baselines in terms of accuracy in most settings but also generates explanations that enable reproducing the behavior of the predictor.



2 Method

2.1 Problem Formulation

We formulate our problem as a supervised graph classification. A graph $G = (V, E)$ has node attributes x_v for $v \in V$ and edge attributes e_{uv} for $(u, v) \in E$. Given a graph set $\mathcal{G} = \{G_1, G_2, \dots, G_n\}$ and continuous or discrete labels $\mathcal{Y} = \{y_1, y_2, \dots, y_n\}$ for each graph respectively, our goal is to learn a function $\hat{f} : \mathcal{G} \rightarrow \mathcal{Y}$ that approximates the labels of unseen graphs.

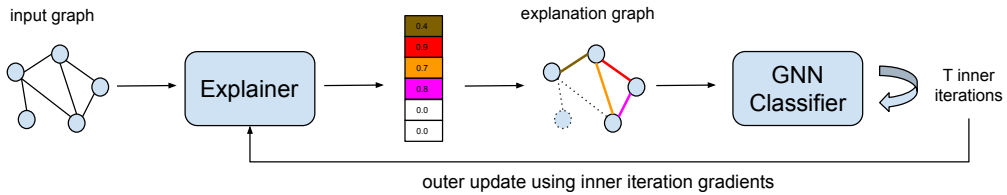
2.2 RAGE: Robust Ante-hoc Graph Explainer

We introduce RAGE, an ante-hoc explainer that generates robust explanations using bilevel optimization. RAGE performs compact and discriminative subgraph learning as part of the GNN training that optimizes the prediction of class labels in graph classification tasks.

RAGE is based on a general scheme for an edge-based approach for learning ante-hoc explanations using bilevel optimization, as illustrated in Figure 3. The explainer will assign an influence value to each edge, which will be incorporated into the original graph. The GNN classifier is trained with this new graph over T inner iterations. Gradients from inner iterations are kept to update the explainer in the outer loop. The outer iterations minimize a loss function that induces explanations to be compact (sparse) and discriminative (accurate). We will now describe our approach (RAGE) in more detail.

2.2.1 Explainer - Subgraph Learning

RAGE is an edge-based subgraph learner. It learns edge representations from edge features and the corresponding node representations/features. Surprisingly, most edge-based explainers for undirected graphs are not permutation invariant when calculating edge representations (e.g., PGExplainer [23] concatenates node representations based on their index order). Shuffling nodes could change their performance drastically since the edge representations would differ. We calculate permutation invariant edge representations h_{ij} given two node representations h_i and h_j as follows: $h_{ij} = [\mathbf{max}(h_i, h_j); \mathbf{min}(h_i, h_j)]$, where \mathbf{max} and \mathbf{min} are pairwise for each dimension and $[\cdot; \cdot]$ is the



concatenation operator. Additionally, most existing explainers do not consider edge features, which are crucial for certain domains such as molecular graphs. Since many recent GNNs readily incorporate edge features [16], we utilize them in processing the input graph to obtain h_i and h_j that take into account both node and edge features.

Edge influences are learned via an MLP with sigmoid activation based on edge representations: $z_{ij} = MLP(h_{ij})$. This generates an edge influence matrix $Z \in [0, 1]^{n \times n}$. We denote our explainer function as g_Φ with trainable parameters Φ .

2.2.2 Influence-weighted Graph Neural Networks

Any GNN architecture can be made sensitive to edge influences Z via a transformation of the adjacency matrix of the input graphs. As our model does not rely on a specific architecture, we will refer to it generically as $GNN(A, X)$, where A and X are the adjacency and attribute matrices, respectively. We rescale the adjacency matrix with edge influences Z as follows: $A_Z = Z \odot A$.

The GNN treats A_Z in the same way as the original matrix: $H = GNN(A_Z, X)$

We generate a graph representation h from the node representation matrix H via a mean pooling operator. The graph representation h is then given as input to a classifier that will predict graph labels y . Here, we use an MLP as our classifier.

2.2.3 Bilevel Optimization

In order to perform both GNN training and estimate the influence of edges jointly, we formulate graph classification as a bilevel optimization problem. In the inner problem (Equation 2), we learn the GNN parameters $\theta^* \in \mathbb{R}^h$ given edges influences $Z^* \in [0, 1]^{n \times n}$ based on a training loss ℓ^{tr} and training data (D^{tr}, y^{tr}) . We use the symbol C to refer to any GNN architecture. In the outer problem (Equation 1), we learn edge influences Z^* by minimizing the loss ℓ^{sup} using support data (D^{sup}, y^{sup}) .

$$Z^* = \arg \min_Z F(\theta^*, Z) = \ell^{sup}(C(\theta^*, Z, D^{sup}), y^{sup}) \quad (1)$$

$$\theta^* = \arg \min_\theta f_{Z^*}(\theta) = \ell^{tr}(C(\theta, Z^*, D^{tr}), y^{tr}) \quad (2)$$

RAGE can be understood through the lens of meta-learning. The outer problem performs *meta-training* and edge influences are learned by a *meta-learner* based on support data. The inner problem solves multiple *tasks* representing different training splits sharing the same influence weights.

At this point, it is crucial to justify the use of bilevel optimization to compute edge influences Z . A simpler alternative would be computing influences as edge attention weights using standard gradient-based algorithms (i.e., single-level). However, we argue that bilevel optimization is a more robust approach to our problem. More specifically, we decouple the learning of edge influences from the GNN parameters and share the same edge influences in multiple training splits. Consequently, these influences are more likely to generalize to unseen data. We validate this hypothesis empirically using different datasets in our experiments in Appendix B.

2.3 Bilevel Optimization Training

The main steps performed by our model (RAGE) are given in Algorithm 1. For each outer iteration (lines 1-13), we split the training data into two sets—training and support—(line 2). First, we use training data to calculate Z^{tr} , which is used for *GNN* training in the inner loop (lines 4-9). Then, we apply the gradients from the inner problem to optimize the outer problem using support data (lines 10-12). The main output of our algorithm is the explainer g_{Φ_κ} . Moreover, the last trained GNN_{θ_T} can also be used for the classification of unseen data or a new GNN can be trained based on Z . In both cases, the GNN will be trained with the same input graphs, which guarantees the behavior of the model GNN_{θ_T} can be reproduced using explanations from g_{Φ_κ} .

For gradient calculation, we follow the gradient-based approach described in [14]. The critical challenge of training our model is how to compute gradients of our outer objective with respect to

Algorithm 1 RAGE

Require: Graphs $A_{1:n}$, node attributes $X_{1:n}$, labels $y_{1:n}$, explainer g_{Φ_0} , outer/inner loops κ and T
Ensure: Trained g_{Φ_κ}

- 1: **for** $\tau \in [0, \kappa - 1]$ **do**
- 2: $A^{tr}, A^{sup}, X^{tr}, X^{sup}, y^{tr}, y^{sup} \leftarrow \text{split}(A_{1:n}, X_{1:n}, y_{1:n})$
- 3: $Z^{tr} \leftarrow g_{\Phi_\tau}(A^{tr}, X^{tr})$
- 4: **for** $t \in [0, T - 1]$ **do**
- 5: $H^{tr} \leftarrow GNN_{\tau, t}(Z^{tr} \odot A^{tr}, X^{tr})$
- 6: $h^{tr} \leftarrow \text{POOL}_{mean}(H^{tr})$
- 7: $p^{tr} \leftarrow \text{MLP}_{\tau, t}(h^{tr})$
- 8: $GNN_{\tau, t+1}, \text{MLP}_{\tau, t+1} \leftarrow \text{inner-opt } f_{Z^{tr}}(p^{tr}, y^{tr})$
- 9: **end for**
- 10: $Z^{sup} \leftarrow g_{\Phi_\tau}(A^{sup}, X^{sup})$
- 11: $p^{sup} \leftarrow \text{MLP}_{\tau, T}(\text{POOL}_{mean}(GNN_{\tau, T}(Z^{sup} \odot A^{sup}, X^{sup})))$
- 12: $g_{\Phi_{\tau+1}} \leftarrow \text{outer-opt } F_{\theta_T}(p^{sup}, y^{sup})$
- 13: **end for**
- 14: **return** g_{Φ_κ}

edge influences Z . By the chain rule, such gradients depend on the gradient of the training loss with respect to Z . We will, again, use the connection between RAGE and meta-learning to describe the training algorithm.

2.3.1 Training (Inner Loop)

At inner loop iterations, we keep gradients while optimizing model parameters θ .

$$\theta_{t+1} = \text{inner-opt}_t(\theta_t, \nabla_{\theta_t} \ell^{tr}(\theta_t, Z_\tau))$$

After T iterations, we compute θ^* , which is a function of $\theta_1, \dots, \theta_T$ and Z_τ , where τ is the number of iterations for meta-training. Here, inner-opt_t is the inner optimization process that updates θ_t at step t . If we use SGD as an optimizer, inner-opt_t will be written as follows with a learning rate η :

$$\text{inner-opt}_t(\theta_t, \nabla_{\theta_t} \ell^{tr}(\theta_t, Z_\tau)) := \theta_t - \eta \cdot \nabla_{\theta_t} \ell^{tr}(\theta_t, Z_\tau)$$

2.3.2 Meta-training (Outer Loop)

After T inner iterations, the gradient trajectory saved to θ^* will be used to optimize Φ . We denote outer-opt_τ as outer optimization that updates Φ_τ at step τ . The meta-training step is written as:

$$\begin{aligned} \Phi_{\tau+1} &= \text{outer-opt}_\tau(\Phi_\tau, \nabla_{\Phi_\tau} \ell^{sup}(\theta^*)) \\ &= \text{outer-opt}_\tau(\Phi_\tau, \nabla_{\Phi_\tau} \ell^{sup}(\text{inner-opt}_T(\theta_T, \nabla_{\theta_T} \ell^{tr}(\theta_T, Z_\tau)))) \end{aligned}$$

After each meta optimization step, we calculate edge influences $Z_{\tau+1}$ using $g_{\Phi_{\tau+1}}(\cdot)$. Our training algorithm is more computationally intensive than training a simple GNN architecture. For that reason, we set T to a small value. Note that both edge influence learning and graph classification use GNNs to produce node and graph representations. These processes can either use separate GNNs or share the same architecture, also known as weight sharing. We found the latter to produce slightly better accuracy. This choice makes sense because intuitively a good subgraph learner is inherently a good classifier. Such a strategy is also employed in [25].

3 Experiments

We evaluate RAGE on several datasets and compare it against both post-hoc and ante-hoc explainers in terms of discriminative power and robustness. A key advantage of our approach is being able to effectively search for a GNN that is both explainable and accurate. We focus our evaluation on molecular graphs, an important domain of graph learning with a wide range of critical scientific applications, such as drug discovery, which greatly benefit from good explanations.

Table 1: Classification performances in AUC of RAGE and other baselines.

Models	Lactam	BenLac	BenLacM	BBBP	ClinTox	Tox21	ToxCast	Mutagenicity
RAGE (ours)	100.0 ± 0.0	99.6 ± 0.7	100.0 ± 0.0	67.1 ± 2.1	85.8 ± 4.2	74.6 ± 0.7	62.1 ± 0.9	87.7 ± 1.6
GSAT	100.0 ± 0.0	99.4 ± 1.6	100.0 ± 0.0	65.8 ± 2.2	87.5 ± 2.7	72.9 ± 0.9	61.4 ± 0.8	82.6 ± 1.3
DIR-GNN	86.8 ± 4.7	89.7 ± 6.8	99.2 ± 0.9	64.4 ± 2.9	79.5 ± 6.0	70.8 ± 0.8	61.2 ± 0.6	84.3 ± 1.5
GIN	100.0 ± 0.0	98.1 ± 3.9	100.0 ± 0.0	65.9 ± 1.9	83.5 ± 5.0	74.3 ± 1.0	61.7 ± 0.7	87.4 ± 1.2
GCN	100.0 ± 0.0	99.3 ± 1.0	100.0 ± 0.0	64.8 ± 2.8	83.4 ± 6.7	73.9 ± 0.6	62.3 ± 1.0	88.0 ± 1.3
GAT	100.0 ± 0.0	98.3 ± 1.8	100.0 ± 0.0	65.1 ± 1.3	82.6 ± 4.5	74.0 ± 0.9	63.2 ± 0.8	87.5 ± 1.4
GMT	100.0 ± 0.0	99.5 ± 0.6	100.0 ± 0.0	65.8 ± 1.9	82.3 ± 1.7	74.0 ± 0.8	62.0 ± 0.7	86.4 ± 1.1
VIB-GSL	88.2 ± 4.2	94.1 ± 4.3	99.6 ± 0.4	67.5 ± 1.9	78.8 ± 2.0	71.5 ± 4.9	61.1 ± 0.5	83.3 ± 1.4

3.1 Datasets

In our experiments, we use a total of 8 graph-based molecular datasets, including 5 real-world classification datasets and 3 synthetic molecular datasets with ground-truth labels that we curated.

Graph Classification Datasets We consider 4 binary graph classification datasets from MoleculeNet [35]: BBBP, CLINTOX, Tox21, and ToxCast. Additionally, we include MUTAGENICITY [18, 6, 27], a popular molecular classification dataset with ground-truth explanations. However, since there is currently no consensus on these explanations [30, 23, 6], we exclude MUTAGENICITY from the evaluation of the explanations produced by RAGE and the baselines.

Constructing Molecular Synthetic Datasets Most graph-based datasets with ground-truth explanations consist of synthetic non-molecular graphs [1]. Evaluating explainer models using these datasets may not reflect the expected behavior of these models in real-world settings (e.g., drug discovery) due to the disparity between synthetic graphs and real-world graphs. Instead, we curate 3 semi-synthetic molecular graph datasets with ground-truth explanations. We screen millions of molecules from the ChEMBL database [12] and extract the ones with either or both of Lactam and Benzoyl functional groups. Lactam groups are cyclic amides with various ring sizes and the Benzoyl group is a benzene ring attached to a carbonyl group. The 3 datasets are defined as follows:

- **LACTAM**: Positive if molecules containing a Lactam group and negative otherwise. There is no molecule with multiple Lactam groups.
- **BenLac** (Benzoyl Lactam): Positive if molecules containing a Lactam group; negative if molecules containing a Benzoyl group, a Lactam group with a Benzoyl group, or no Lactam and Benzoyl groups. There is no molecule with multiple Lactam or Benzoyl groups.
- **BenLacM** (Benzoyl Lactam Multiclass): Class I if molecules containing a Lactam group; class II if molecules containing a Benzoyl group. Each molecule has either a Lactam or a Benzoyl group. We do not term the labels positive or negative since there is no class of interest in this setting.

One favorable aspect of these datasets is that the prediction is simple for most classifiers yet the explanation is not trivial, as we show in Section 3.3 and Section 3.4. This property allows us to assess not only the quality of the explanation but also the ability of the classifier to pick up the right signals from data. Both aspects are important for RAGE and ante-hoc explainers as both the explanations and the classifier are learned together. More details on these datasets are provided in Appendix A.

3.2 Experimental Settings

Baselines We compare RAGE against a variety of baselines in terms of both classification and explanation abilities. For classification, we include classical models such as GCN [19], GAT [31], and GIN [37]. We also include GMT [2], a state-of-the-art GNN with attention-based graph pooling, and VIB-GSL [29], a method that applies graph structure learning. For explanations on the semi-synthetic molecular datasets, we compare RAGE against both inductive explainers (e.g., PGExplainer [23], GEM [22]) and transductive explainers (e.g., GNNExplainer [39], CFF [30]). Most importantly, we compare RAGE against existing ante-hoc graph explainers such as GSAT [25] and DIR-GNN [34].

Models and Training For GSAT, we follow the configuration suggested by the authors for OGB datasets [25]. For DIR-GNN [34] and VIB-GSL [29], we try our best to finetune the models. For

Table 2: Performance of RAGE and other baselines on explainability.

Models	Lactam		BenLac		BenLacM	
	ExAUC	Precision@10	ExAUC	Precision@10	ExAUC	Precision@10
RAGE (ours)	98.2 ± 1.6	<u>85.9 ± 6.8</u>	<u>81.7 ± 7.9</u>	87.0 ± 8.4	92.9 ± 2.8	83.6 ± 3.6
GSAT	<u>97.7 ± 1.9</u>	80.1 ± 6.7	84.5 ± 8.3	<u>73.5 ± 10.6</u>	74.1 ± 7.5	71.2 ± 11.5
PGExplainer	96.9 ± 0.8	87.4 ± 4.1	73.3 ± 1.9	71.6 ± 2.6	<u>86.5 ± 1.8</u>	<u>81.0 ± 0.1</u>
GNNExplainer	80.1 ± 1.7	50.8 ± 3.4	51.7 ± 1.1	65.2 ± 6.8	<u>57.6 ± 0.8</u>	36.4 ± 1.5
GEM	68.1 ± 11.1	48.4 ± 17.9	55.0 ± 6.2	56.5 ± 8.9	<u>56.6 ± 5.8</u>	42.0 ± 5.5
CFF	93.5 ± 0.6	81.4 ± 1.3	50.7 ± 0.9	50.4 ± 2.3	<u>51.4 ± 0.8</u>	38.9 ± 1.2

any baseline that does not support edge features, we replace their GNN implementation with ours. Specifically, for fair and consistent comparisons, we choose GIN [37] with edge encodings as the backbone of all explainers. Following the experiments from previous works [15] on molecular datasets, we construct the GIN backbone with 5 layers and 300 hidden dimensions. We also keep this architectural setting for other GNN baselines, including GCN [19], GAT [31], and GMT [2]. For post-hoc baselines, we obtain their performances via GNN-X-Bench [20]. For our experiments on RAGE, we use Adam optimizer, batch size 256, learning rate $1e - 4$, and weight decay 0. All datasets are split with the 8:1:1 ratio for train, validation, and test splits. All experiments are conducted on a shared computing server with random access to either Nvidia V100 or A100 GPUs.

3.3 Results on Graph Classification

Table 1 shows the results of RAGE and other baselines on chemical classification benchmarks. For each dataset, we report the mean AUC and error from 10 runs. The best performance on each dataset is bolded and the second best performance is underscored. We do not show these highlights for LACTAM, BENLAC, and BENLACM because most baselines obtain near-perfect classification on these semi-synthetic datasets. Nevertheless, these datasets are meant for comparing the explanation ability and perfect classification performances promote better comparison of the extracted explanations. We include them in Table 1 for the sake of completeness.

No single baseline obtains the best performance on more than one dataset. RAGE is the best classifier for TOX21 while ante-hoc GSAT [25] performs the best on CLINTOX. Substructure learner VIB-GSL [29] does particularly well on BBBP but not on other benchmarks. In terms of overall competitiveness, our method RAGE is among the top 2 performing models on 4 out of the 5 reported real-world chemical datasets. Notice that RAGE performs better than its backbone model GIN [37] across all chemical benchmarks, confirming the effectiveness of our framework as a classifier.

3.4 Results on Explainability

In Table 2, we show the explanation performances of RAGE and other explainers on the 3 semi-synthetic molecular datasets. Two important metrics, explanation AUC and precision among the top 10 weighted edges, are reported based on the ground-truth subgraphs. We compare RAGE directly with GSAT [25], a strong ante-hoc baseline. We also include post-hoc explainers of which explanations are based on the trained GIN models obtained from the graph classification experiment. We use all graphs in calculating explanation AUCs and only use graphs with ground-truth explanations in calculating precisions. For more details about ground-truth explanations, refer to Appendix A.

Across the datasets, RAGE performs competitively both in terms of explanation AUC and precision. Remarkably, on the multiclass dataset BENLACM, our method is the best in both metrics. On LACTAM, RAGE obtains the best explanation AUC and the second best precision while on BENLAC, we achieve the best precision and second best explanation AUC. The results suggest that ante-hoc methods like RAGE and GSAT generally do better than post-hoc alternatives, among which we find PGExplainer to be the most competitive.

Figure 4 visualizes the edge weights assigned by RAGE and GSAT. The green density plots show weights assigned to edges belonging to the ground-truth explanations (foreground edges) while the pink density plots show the same for the remaining edges (background edges). Notice that since the semi-synthetic datasets are highly skewed, the actual density of foreground edges would be much

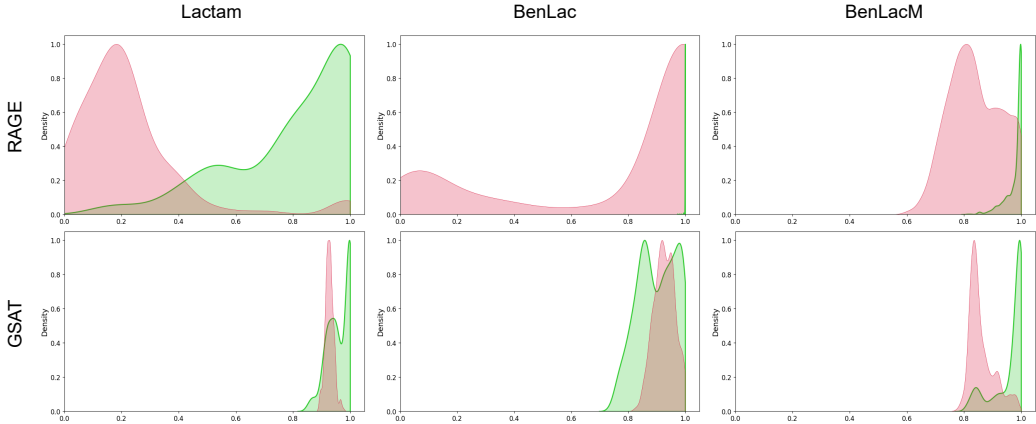


Figure 4: Comparisons between the absolute weights assigned by RAGE and GSAT on ground-truth explanation (foreground) edges and the remaining (background) edges. The plots illustrate the density of edge weights across 3 synthetic molecular datasets. Densities of foreground edge weights are shown in green while those of background edge weights are shown in pink. The density of foreground edges by RAGE on BENLAC is barely visible because most foreground weights are close to 1.0.

smaller than that of background edges, however, for clarity, we normalize all plots. For GSAT, the weights assigned to either foreground edges and background edges are quite close to each other while RAGE tends to assign lower weights to background edges. In BENLAC, RAGE assigns weights close to 1.0 most foreground edges, which results in a density plot that looks like a vertical line.

3.5 Reproducibility

Reproducibility measures how explanations alone can predict class labels. It is a key property as it allows users to correlate explanations and predictions without neglecting potentially relevant information from the input. We vary the size of the explanations by thresholding edges based on their importance. We then train a GNN using only the explanations and labels. We compare RAGE against post-hoc and ante-hoc explainers on MUTAGENICITY and show the results in Figure 5.

The results demonstrate that RAGE outperforms competing explainers in terms of reproducibility. Ante-hoc methods, RAGE and GSAT, emerge as the best and second best methods, confirming the superiority of ante-hoc learning in terms of generalization and robustness. RAGE incorporates these qualities through meta-training and bilevel optimization. Two post-hoc explainers, PGExplainer and GNNExplainer, perform poorly. As expected, larger explanations lead to better reproducibility.

3.6 Ablation Study

We include ablation experiments investigating the effects of varying the number of inner iterations and the backbone GNN on the performances of RAGE. The details can be found in Appendix B.

4 Related Works

Graph classification with GNNs: Graph Neural Networks (GNNs) have gained prominence in graph classification due to their ability to learn features directly from data [19, 31, 13, 37]. GNN-based graph classifiers aggregate node-level representations via pooling operators to represent the entire graph. The design of effective graph pooling operators is key for effective graph classification [40, 44, 21, 11, 24]. Recently, [2] proposed a multi-head attention pooling layer to capture structural dependencies between nodes. In this paper, we focus on graph classification and show that our approach achieves competitive discriminative power compared to that of state-of-the-art alternatives [37, 2] while at the same time producing robust explanations.

Explainability of GNNs: Explainability has become a key requirement for the application of machine learning in many settings (e.g., healthcare, court decisions, scientific discoveries) [26]. Several

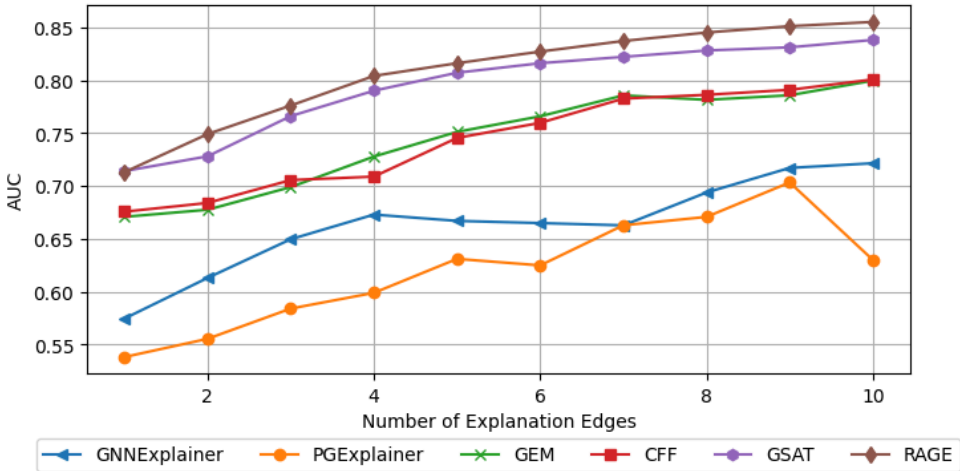


Figure 5: Reproducibility of various ante-hoc and post-hoc explainers on Mutagenicity. We extracted explanation subgraphs by keeping the edges with the highest weights and trained a classifier on the resulting dataset comprising these subgraphs. RAGE and GSAT, being ante-hoc, perform better than other post-hoc explainers under such perturbation.

post-hoc explainers have been proposed for explaining Graph Neural Networks’ predictions using subgraphs [39, 23, 43, 3, 30, 36]. GNNExplainer [39] applies a mean-field approximation to identify subgraphs that maximize the mutual information with GNN predictions. PGExplainer [23] applies a similar objective, but samples subgraphs using the *reparametrization trick*. RCEExplainer [3] generates counterfactual subgraph explanations. While post-hoc explainers treat a trained GNN as a black box —i.e., it only relies on predictions made by the GNN—ante-hoc explainers are model-dependent. DIR-GNN trains an intrinsically explainable GNN by discovering and generating label-invariant rationales (subgraphs). GIB [41] applies the *bottleneck principle* and bilevel optimization to learn subgraphs relevant for classification but different from the corresponding input graph. GSAT [25], in an end-to-end fashion, combines information bottleneck with attention to sample explanation graphs as inputs into a classifier. This approach is the most related to our framework. We compare RAGE and GSAT rigorously in all experiments, in which RAGE outperforms the latter in various scenarios. However, the end-to-end training that GSAT employs is faster than our bilevel optimization. We discuss more about this limitation in Appendix D. Nevertheless, RAGE is competitive in terms of training and testing time compared to other GNN and explainer baselines (Appendix C).

Bilevel optimization: Bilevel optimization is a class of optimization problems where two objective functions are nested within each other [4]. Although the problem is known to be NP-hard, recent algorithms have enabled the solution of large-scale problems in machine learning, such as automatic hyperparameter optimization and meta-learning [9]. Bilevel optimization has also been applied to graph problems, including graph meta-learning [17] and transductive graph sparsification [33].

Graph structure learning: Graph structure learning (GSL) aims to enhance (e.g., complete, denoise) graph information to improve the performance of downstream tasks [46]. LDS-GNN [10] applies bilevel optimization to learn the graph structure that optimizes node classification. VIB-GSL [29] advances GIB [41] by applying a variational information bottleneck on the entire graph instead of only edges. We notice that GSL mainly focuses on learning the entire graph, whereas we only sparsify the graph, which reduces the search space and is more interpretable than possibly adding new edges. Furthermore, learning the entire graph is not scalable in large graph settings.

5 Conclusion

We investigated the problem of generating explanations for GNN-based graph-level classification and proposed RAGE, a novel ante-hoc GNN explainer based on bilevel optimization. RAGE inductively learns compact and accurate explanations by optimizing the GNN and explanations jointly. Moreover,

different from several baselines, RAGE explanations do not omit any information used by the model, thus enabling the model behavior to be reproduced based on the explanations. We compared RAGE against state-of-the-art graph classification methods and GNN explainers using synthetic and real datasets. The results show that RAGE often outperforms the baselines on multiple evaluation metrics, including accuracy and robustness.

Acknowledgments and Disclosure of Funding

Mert Kosan worked on this project prior to joining Visa Inc.

References

- [1] Chirag Agarwal, Owen Queen, Himabindu Lakkaraju, and Marinka Zitnik. Evaluating explainability for graph neural networks. *Scientific Data*, 10(1):144, 2023.
- [2] Jinheon Baek, Minki Kang, and Sung Ju Hwang. Accurate learning of graph representations with graph multiset pooling. In *ICLR*, 2021.
- [3] Mohit Bajaj, Lingyang Chu, Zi Yu Xue, Jian Pei, Lanjun Wang, Peter Cho-Ho Lam, and Yong Zhang. Robust counterfactual explanations on graph neural networks. *Advances in Neural Information Processing Systems*, 34:5644–5655, 2021.
- [4] Benoît Colson, Patrice Marcotte, and Gilles Savard. An overview of bilevel optimization. *Annals of operations research*, 153(1):235–256, 2007.
- [5] Mathieu Dagréou, Pierre Ablin, Samuel Vaïter, and Thomas Moreau. A framework for bilevel optimization that enables stochastic and global variance reduction algorithms. *Advances in Neural Information Processing Systems*, 35:26698–26710, 2022.
- [6] Asim Kumar Debnath, Rosa L Lopez de Compadre, Gargi Debnath, Alan J Shusterman, and Corwin Hansch. Structure-activity relationship of mutagenic aromatic and heteroaromatic nitro compounds. correlation with molecular orbital energies and hydrophobicity. *Journal of medicinal chemistry*, 34(2):786–797, 1991.
- [7] Youran Dong, Shiqian Ma, Junfeng Yang, and Chao Yin. A single-loop algorithm for decentralized bilevel optimization. *arXiv preprint arXiv:2311.08945*, 2023.
- [8] Lukas Faber, Amin K Moghaddam, and Roger Wattenhofer. Contrastive graph neural network explanation. In *ICML Workshop on Graph Representation Learning and Beyond*, page 28. International Conference on Machine Learning, 2020.
- [9] Luca Franceschi, Paolo Frasconi, Saverio Salzo, Riccardo Grazzi, and Massimiliano Pontil. Bilevel programming for hyperparameter optimization and meta-learning. In *International Conference on Machine Learning*, pages 1568–1577. PMLR, 2018.
- [10] Luca Franceschi, Mathias Niepert, Massimiliano Pontil, and Xiao He. Learning discrete structures for graph neural networks. In *International conference on machine learning*, pages 1972–1982. PMLR, 2019.
- [11] Hongyang Gao and Shuiwang Ji. Graph u-nets. In *international conference on machine learning*, pages 2083–2092. PMLR, 2019.
- [12] Anna Gaulton, Louisa J Bellis, A Patricia Bento, Jon Chambers, Mark Davies, Anne Hersey, Yvonne Light, Shaun McGlinchey, David Michalovich, Bissan Al-Lazikani, et al. Chembl: a large-scale bioactivity database for drug discovery. *Nucleic acids research*, 40(D1):D1100–D1107, 2012.
- [13] Justin Gilmer, Samuel S Schoenholz, Patrick F Riley, Oriol Vinyals, and George E Dahl. Neural message passing for quantum chemistry. In *International conference on machine learning*, pages 1263–1272. PMLR, 2017.
- [14] Edward Grefenstette, Brandon Amos, Denis Yarats, Phu Mon Htut, Artem Molchanov, Franziska Meier, Douwe Kiela, Kyunghyun Cho, and Soumith Chintala. Generalized inner loop meta-learning. *arXiv preprint arXiv:1910.01727*, 2019.
- [15] Weihua Hu, Matthias Fey, Marinka Zitnik, Yuxiao Dong, Hongyu Ren, Bowen Liu, Michele Catasta, and Jure Leskovec. Open graph benchmark: Datasets for machine learning on graphs. *Advances in neural information processing systems*, 33:22118–22133, 2020.

[16] Weihua Hu, Bowen Liu, Joseph Gomes, Marinka Zitnik, Percy Liang, Vijay Pande, and Jure Leskovec. Strategies for pre-training graph neural networks. In *International Conference on Learning Representations*, 2020.

[17] Kexin Huang and Marinka Zitnik. Graph meta learning via local subgraphs. *Advances in Neural Information Processing Systems*, 33, 2020.

[18] Jeroen Kazijs, Ross McGuire, and Roberta Bursi. Derivation and validation of toxicophores for mutagenicity prediction. *Journal of medicinal chemistry*, 48(1):312–320, 2005.

[19] Thomas N Kipf and Max Welling. Semi-supervised classification with graph convolutional networks. *arXiv preprint arXiv:1609.02907*, 2016.

[20] Mert Kosan, Samidha Verma, Burouj Armgaaan, Khushbu Pahwa, Ambuj Singh, Sourav Medya, and Sayan Ranu. Gnnx-bench: Unravelling the utility of perturbation-based gnn explainers through in-depth benchmarking. In *The Twelfth International Conference on Learning Representations*, 2023.

[21] Jia Li, Yu Rong, Hong Cheng, Helen Meng, Wenbing Huang, and Junzhou Huang. Semi-supervised graph classification: A hierarchical graph perspective. In *The Web Conference*, pages 972–982, 2019.

[22] Wanyu Lin, Hao Lan, and Baochun Li. Generative causal explanations for graph neural networks. In *International Conference on Machine Learning*, pages 6666–6679. PMLR, 2021.

[23] Dongsheng Luo, Wei Cheng, Dongkuan Xu, Wenchao Yu, Bo Zong, Haifeng Chen, and Xiang Zhang. Parameterized explainer for graph neural network. *arXiv preprint arXiv:2011.04573*, 2020.

[24] Diego Mesquita, Amauri Souza, and Samuel Kaski. Rethinking pooling in graph neural networks. *Advances in Neural Information Processing Systems*, 33:2220–2231, 2020.

[25] Siqi Miao, Mia Liu, and Pan Li. Interpretable and generalizable graph learning via stochastic attention mechanism. In *International Conference on Machine Learning*, pages 15524–15543. PMLR, 2022.

[26] Christoph Molnar. *Interpretable machine learning*. Lulu. com, 2020.

[27] Christopher Morris, Nils M Kriege, Franka Bause, Kristian Kersting, Petra Mutzel, and Marion Neumann. Tudataset: A collection of benchmark datasets for learning with graphs. *arXiv preprint arXiv:2007.08663*, 2020.

[28] Cynthia Rudin. Stop explaining black box machine learning models for high stakes decisions and use interpretable models instead. *Nature Machine Intelligence*, 1(5):206–215, 2019.

[29] Qingyun Sun, Jianxin Li, Hao Peng, Jia Wu, Xingcheng Fu, Cheng Ji, and S Yu Philip. Graph structure learning with variational information bottleneck. In *Proceedings of the AAAI Conference on Artificial Intelligence*, volume 36, pages 4165–4174, 2022.

[30] Juntao Tan, Shijie Geng, Zuohui Fu, Yingqiang Ge, Shuyuan Xu, Yunqi Li, and Yongfeng Zhang. Learning and evaluating graph neural network explanations based on counterfactual and factual reasoning. In *Proceedings of the ACM Web Conference 2022*, pages 1018–1027, 2022.

[31] Petar Veličković, Guillem Cucurull, Arantxa Casanova, Adriana Romero, Pietro Lio, and Yoshua Bengio. Graph attention networks. *arXiv preprint arXiv:1710.10903*, 2017.

[32] Giulia Vilone and Luca Longo. Explainable artificial intelligence: a systematic review. *arXiv preprint arXiv:2006.00093*, 2020.

[33] Guihong Wan and Haim Schweitzer. Edge sparsification for graphs via meta-learning. In *2021 IEEE 37th International Conference on Data Engineering (ICDE)*, pages 2733–2738. IEEE, 2021.

[34] Yingxin Wu, Xiang Wang, An Zhang, Xiangnan He, and Tat-Seng Chua. Discovering invariant rationales for graph neural networks. In *International Conference on Learning Representations*, 2021.

[35] Zhenqin Wu, Bharath Ramsundar, Evan N Feinberg, Joseph Gomes, Caleb Geniesse, Aneesh S Pappu, Karl Leswing, and Vijay Pande. Moleculenet: a benchmark for molecular machine learning. *Chemical science*, 9(2):513–530, 2018.

[36] Yaochen Xie, Sumeet Katariya, Xianfeng Tang, Edward Huang, Nikhil Rao, Karthik Subbian, and Shuiwang Ji. Task-agnostic graph explanations. *arXiv preprint arXiv:2202.08335*, 2022.

- [37] Keyulu Xu, Weihua Hu, Jure Leskovec, and Stefanie Jegelka. How powerful are graph neural networks? *arXiv preprint arXiv:1810.00826*, 2018.
- [38] Junjie Yang, Kaiyi Ji, and Yingbin Liang. Provably faster algorithms for bilevel optimization. *Advances in Neural Information Processing Systems*, 34:13670–13682, 2021.
- [39] Rex Ying, Dylan Bourgeois, Jiaxuan You, Marinka Zitnik, and Jure Leskovec. Gnnexplainer: Generating explanations for graph neural networks. *Advances in neural information processing systems*, 32:9240, 2019.
- [40] Rex Ying, Jiaxuan You, Christopher Morris, Xiang Ren, William L Hamilton, and Jure Leskovec. Hierarchical graph representation learning with differentiable pooling. *arXiv preprint arXiv:1806.08804*, 2018.
- [41] Junchi Yu, Tingyang Xu, Yu Rong, Yatao Bian, Junzhou Huang, and Ran He. Graph information bottleneck for subgraph recognition. In *International Conference on Learning Representations*, 2021.
- [42] Hao Yuan, Haiyang Yu, Shurui Gui, and Shuiwang Ji. Explainability in graph neural networks: A taxonomic survey. *IEEE Transactions on Pattern Analysis and Machine Intelligence*, 2022.
- [43] Hao Yuan, Haiyang Yu, Jie Wang, Kang Li, and Shuiwang Ji. On explainability of graph neural networks via subgraph explorations. In *International Conference on Machine Learning*, pages 12241–12252. PMLR, 2021.
- [44] Muhan Zhang, Zhicheng Cui, Marion Neumann, and Yixin Chen. An end-to-end deep learning architecture for graph classification. In *Proceedings of the AAAI conference on artificial intelligence*, volume 32, 2018.
- [45] Zaixi Zhang, Qi Liu, Hao Wang, Chengqiang Lu, and Cheekong Lee. Protgnn: Towards self-explaining graph neural networks. In *Proceedings of the AAAI Conference on Artificial Intelligence*, volume 36, pages 9127–9135, 2022.
- [46] Yanqiao Zhu, Weizhi Xu, Jinghao Zhang, Qiang Liu, Shu Wu, and Liang Wang. Deep graph structure learning for robust representations: A survey. *arXiv preprint arXiv:2103.03036*, 2021.

A Dataset Details

A.1 Graph Classification Benchmarks

We provide more details about the datasets used in our study. Table 3 and Table 4 show statistics regarding the classification benchmarks and our semi-synthetic datasets, respectively. All benchmarks are medium-size molecular graph datasets with both node features and edge features.

Table 3: Molecular Classification Benchmarks

Datasets	Number of Graphs	Number of Tasks	Number of Node Features	Number of Edge Features
BBBP	2039	1	9	3
ClinTox	1478	2	9	3
Tox21	7831	12	9	3
ToxCast	8575	617	9	3
Mutagenicity	4337	1	14	3

The molecular graph classification datasets reflect real-world applications of graph learning in chemistry. Most of them are obtained from the MoleculeNet [35] with featurization following that of Open Graph Benchmark [15]. In particular, there are 9 node features and 3 edge features describing various atom and bond properties. The Mutagenicity dataset is obtained from TUDataset [27]. In Mutagenicity, the node features and edge features are one-hot encodings of atom types and bond types. More specific descriptions of the datasets and the tasks are as follows:

- BBBP: Blood-brain barrier permeability.
- ClinTox: Drugs that failed clinical trials for toxicity reasons
- Tox21: Toxicology on 12 biological targets
- ToxCast: Toxicology measurements via high-throughput screening
- Mutagenicity: Ability of an agent to cause genetic mutations

A.2 Semi-synthetic Molecular Benchmarks

We introduce 3 semi-synthetic molecular datasets with ground-truth labels (Table 4). Specifically, we screen millions of real molecules from ChEMBL [12] and randomly sample those with Lactam and/or Benzoyl substructures. Both of these functional groups are known to exhibit pharmaceutical values such as anti-bacterial effects. Additionally, lactam groups may have varying sizes, which is interesting as ground-truth explanations. The screening and processing are done via RDKit. Next, we describe the semi-synthetic datasets in more details.

LACTAM is a binary classification dataset to distinguish between molecules containing lactam groups and those not containing the lactam groups, with the former and the latter having the positive and negative labels, respectively. Benzoyl Lactam (BENLAC) is also for binary classification but is a more challenging version of LACTAM. In BENLAC, we consider both the lactam and the benzoyl functional groups. Molecules may contain only lactam groups, only benzoyl groups, both lactam and benzoyl groups, or none of those groups. Out of these molecules, only those containing only lactam groups

Table 4: Semi-synthetic Molecular Benchmarks with Ground-truth Explanations.

Dataset	Task Type	Graph Type	Number of Graphs	Edge Label	Class
Lactam	Binary	w lactam groups	200	Yes	Positive
		w/o lactam groups	1000	No	Negative
BenLac	Binary	w lactam groups only	100	Yes	Positive
		w benzoyl groups only	100	Yes	Negative
		w both lactam and benzoyl groups	200	Yes	Negative
		w/o either lactam or benzoyl groups	800	No	Negative
BenLacM	Multiclass	w lactam groups only	500	Yes	1
		w benzoyl groups only	500	Yes	2

Table 5: Ablation study on varying the GNN backbones and the number of inner epochs. The study is done on chemical classification benchmark with results shown in AUC.

Models	BBBP	ClinTox	Tox21	ToxCast
GIN ₁	66.8 ± 3.3	84.9 ± 4.3	72.8 ± 1.1	61.0 ± 1.5
GCN ₁	66.5 ± 2.3	78.2 ± 5.2	74.1 ± 0.7	61.9 ± 2.7
GIN ₅	67.1 ± 2.1	85.8 ± 4.2	74.6 ± 0.7	62.1 ± 0.9
GCN ₅	66.2 ± 1.8	85.2 ± 4.1	74.3 ± 0.6	62.5 ± 1.9
GIN ₁₀	66.6 ± 2.4	85.7 ± 7.4	73.9 ± 1.0	62.0 ± 1.3
GCN ₁₀	65.2 ± 1.7	82.3 ± 9.2	74.6 ± 0.9	62.6 ± 1.4

Table 6: Ablation study on training with and without bilevel optimization. Classification results are shown in AUC. RAGE with bilevel optimization outperforms RAGE-single in every dataset.

Models	BBBP	ClinTox	Tox21	ToxCast
RAGE (w bilevel optimization)	67.1 ± 2.1	85.8 ± 4.2	74.6 ± 0.7	62.1 ± 0.9
RAGE-single (w/o bilevel optimization)	60.0 ± 3.8	67.3 ± 6.0	65.3 ± 2.4	53.3 ± 2.1

are the positive class. Benzoyl Lactam Multiclass BENLACM is a multiclass classification dataset. BENLACM requires distinguishing between molecules with either lactam groups or benzoyl groups. In this case, both classes have ground-truth explanations. Since most datasets on explainability consider binary classification with ground-truth explanations only for one class of interest, we believe it is interesting to look into scenarios in which different classes of data possesses different explanations. These datasets have the same node and edge featurizations as those of the MoleculeNet [35] benchmarks (e.g BBBP).

B Ablation Study

B.1 Varying the Number of Inner Epochs and the Backbone GNN

In Table 5, we show the classification results in AUC of multiple RAGE trainings with different backbone GNNs and number of inner iterations. Except for BBBP, RAGE with multiple inner epochs tend to perform better than RAGE with only one inner epoch. Interestingly, more epochs do not guarantee equal or better performances. For example, RAGE with GIN backbone achieves the best AUC on Tox21 using 5 inner epochs. The same observation holds for RAGE with GCN on BBBP and CLINTOX. These observations suggest that the number of inner epochs is an important hyperparameter that should be carefully tuned in order to obtain the best performance when learning and explaining with RAGE. Since more inner epochs mean longer training time, depending on the use case, one might opt for less inner epochs, possible trading some diminishing performance gain for significantly better efficiency.

There is no clear winner between GIN and GCN as backbone GNNs. RAGE with GIN does better on BBBP and CLINTOX while RAGE with GCN does better on Tox21 and ToxCast. For that reason, it is important to experiment with multiple types of backbone graph learner for optimal results on any specific use case.

B.2 Learning With and Without Bilevel Optimization

We create a single-level version of RAGE (RAGE-single) to test the effectiveness of our bilevel optimization scheme. More specifically, RAGE-single optimizes the explainer and GNN classifier parts in an end-to-end fashion with a single loss function. Table 6 shows that RAGE consistently outperforms RAGE-single. The performance gap is prominent across all chemical classification benchmarks. These observations confirm the effectiveness and necessity of meta-training and bilevel optimization in our framework.

C Running Time

Bilevel optimization needs more training time than the standard GNNs. Table 7 shows training and testing times on the LACTAM dataset for all methods. For training, we show, in seconds, the amount of time required to finish one training epoch while for testing, we show the amount of time taken to evaluate the whole test split. We do not include training time for GNNExplainer, GEM, and CFF since these are transductive models. Instead, we report, as testing time, the amount of time it take for these methods to fit and explain every graph in the testing set.

RAGE trains slower than standard and some of the sophisticated GNN methods, while having comparable or faster testing time. For post-hoc graph explainers, RAGE is much faster in testing. For ante-hoc explainers, RAGE is slower than in training than GSAT, is the same in testing compared to GSAT, and is significantly faster than DIR-GNN in both training and testing.

Table 7: Training and testing time for RAGE and baselines for LACTAM.

		Training (s/epoch)	Testing (s/fold)
Standard GNNs	GCN	0.165s	0.021s
	GAT	0.216s	0.022s
	GIN	0.203s	0.021s
Sophisticated GNNs	GMT	0.268s	0.027s
	VIB-GSL	40.017s	7.266s
Post-hoc Explainers	PGExplainer	78.026s	1.212s
	GNNExplainer	N/A	111.842s
	GEM	N/A	88.401s
	CFF	N/A	2306.452s
Ante-hoc Explainers	GSAT	0.331s	0.025s
	DIR-GNN	47.017s	6.306s
Our method	RAGE	3.252s	0.025s

D Limitations

The most critical limitation of RAGE is the training time (Table 7), as we rely on bilevel optimization. Even though our inference time is quite efficient, long training time is still a problem in scenario such as online learning or lifelong learning. We expect this problem to be alleviated by applying more efficient bilevel optimization methods, such as those that apply stochastic samplings, decentralized processing, or single-loop algorithms [38, 5, 7]. However, we did not experiment with different meta-learning or bilevel optimization approaches in our study and would like to leave this task for future work.

E More Examples of Explanations

We include more examples of the explanations discovered by RAGE. Figure 6, Figure 7, and Figure 8 show examples from LACTAM, BENLAC, and BENLACM, respectively. In these examples, blue highlights indicate ground-truth explanations and red highlights indicate edge importance learned by RAGE. Darker shades of red mean higher weights.

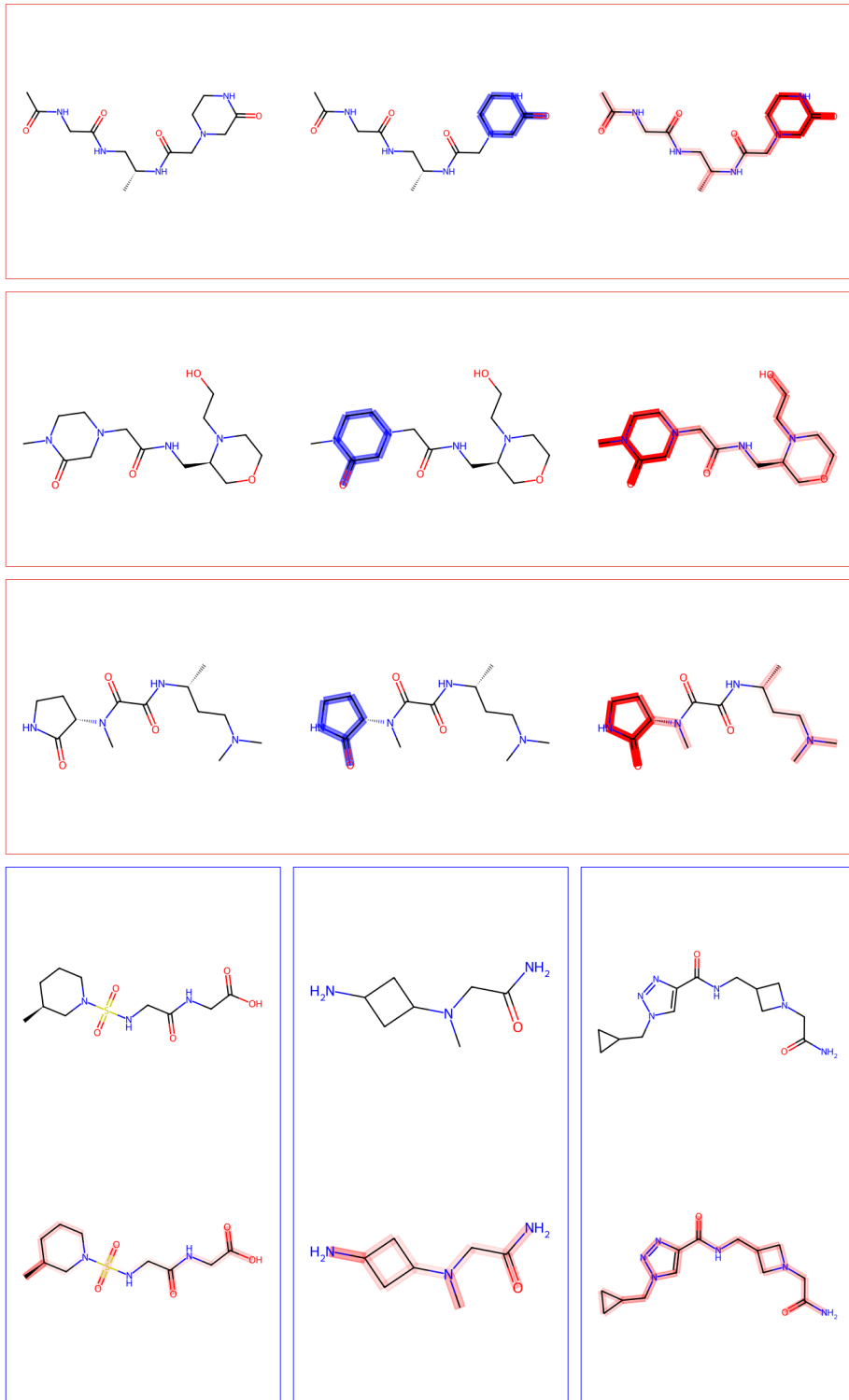


Figure 6: Examples of explanations by RAGE on LACTAM. Positive examples with ground-truth explanations are shown in red boxes and negative examples are shown in blue box.

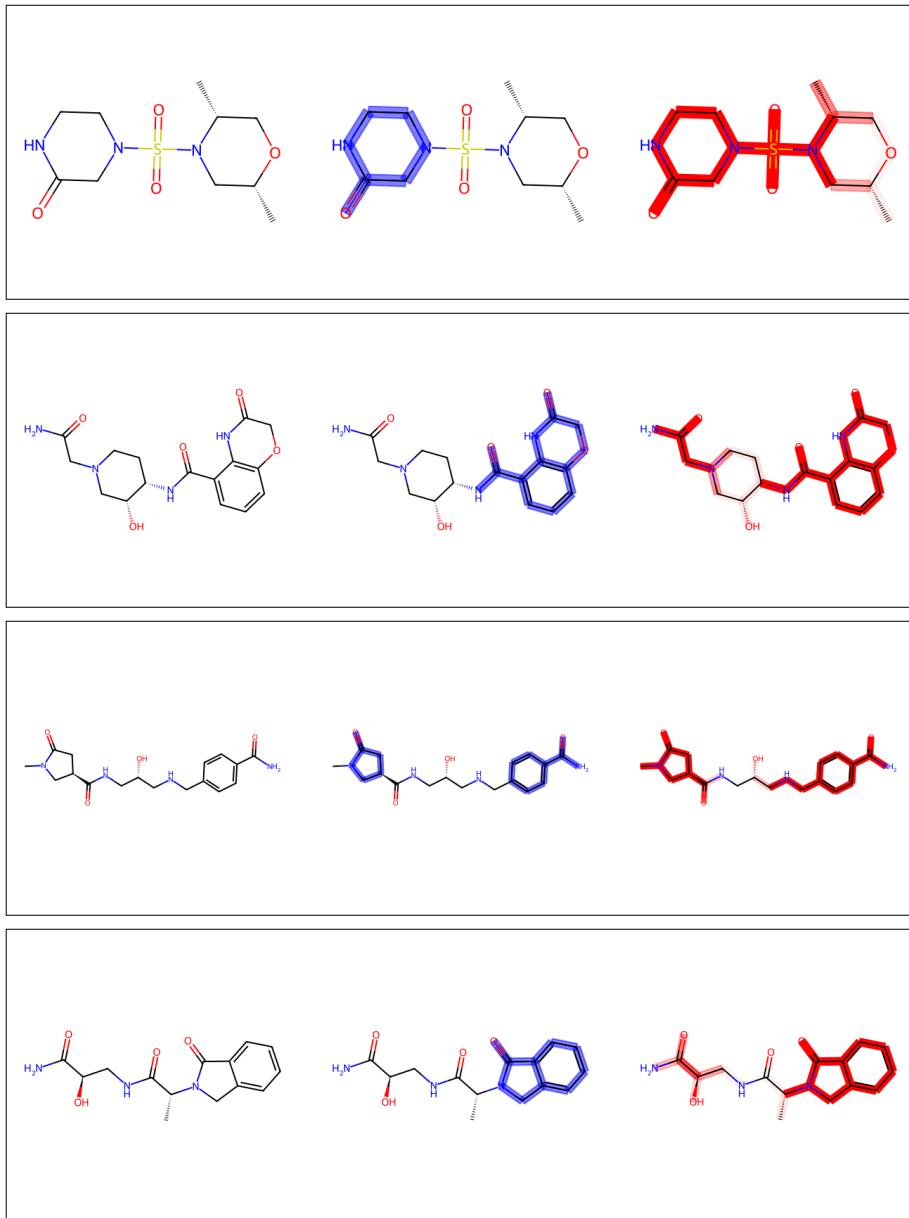


Figure 7: Examples of explanations by RAGE on BENLAC.

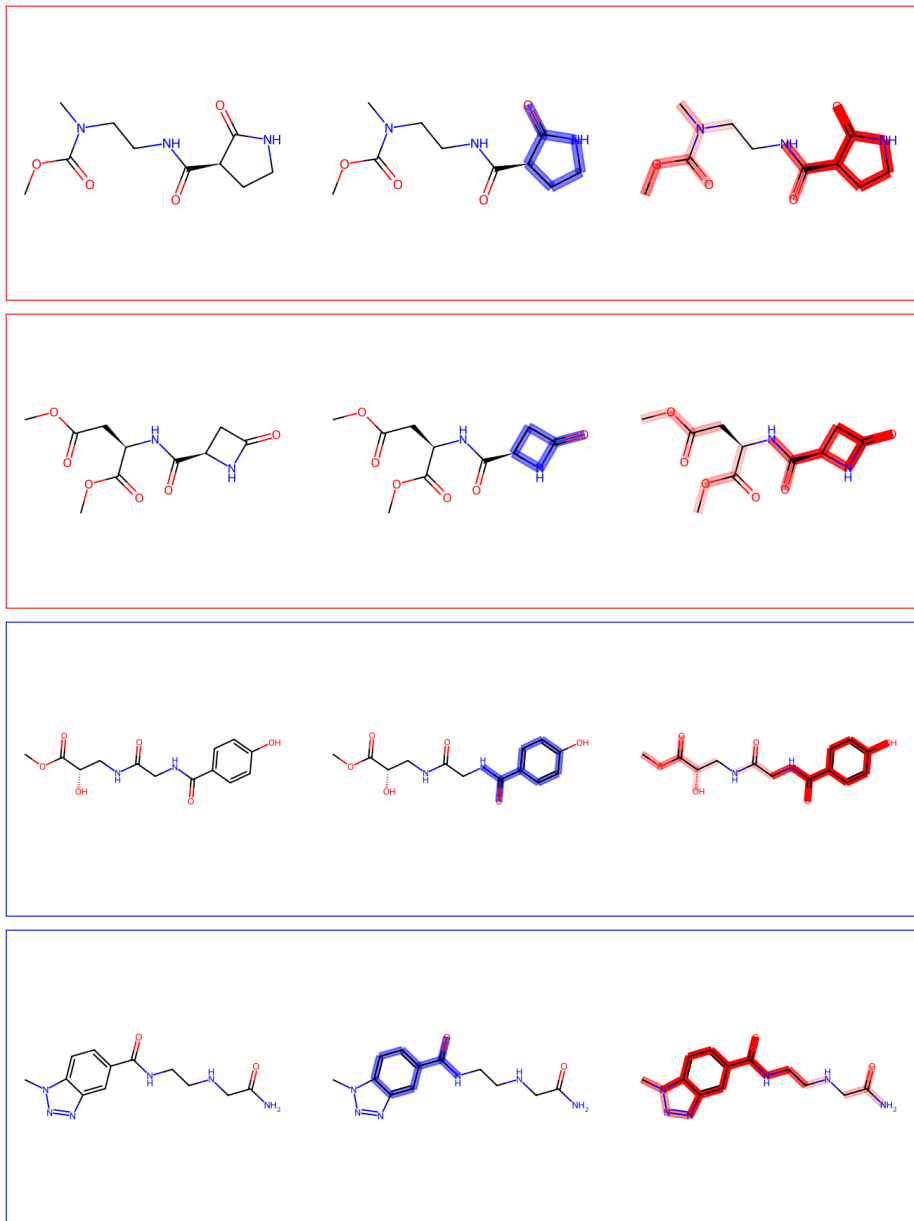


Figure 8: Examples of explanations by RAGE on BENLACM. Red boxes and blue boxes distinguish examples from the 2 classes. Specifically for this dataset, we apply min-max scaling on the weights assigned by RAGE before plotting for better perceptibility.